Design of 3.3 and 4.2 μm mid-infrared metamorphic quantum well light-emitting diodes

Reza Arkani[1,2,*], Christopher A. Broderick[1,2], and Eoin P. O'Reilly[1,2]
[1]Tyndall National Institute, Lee Maltings, Dyke Parade, Cork T12 R5CP, Ireland
[2]Department of Physics, University College Cork, Cork T12 YN60, Ireland
[*]Email: r.arkani@umail.ucc.ie

***Abstract*—The use of $Al_zIn_{1-z}As$ metamorphic buffer layers to facilitate the growth of lattice-mismatched $InN_y(As_{1-x}Sb_x)_{1-y}$ quantum wells on GaAs or InAs substrates has recently been demonstrated to constitute an attractive approach to developing light-emitting devices at application-rich mid-infrared wavelengths. However, little information is available regarding the fundamental properties of this newly established platform. We present a theoretical investigation and optimisation of the properties and performance of $InN_y(As_{1-x}Sb_x)_{1-y}/Al_zIn_{1-z}As$ structures designed to emit at 3.3 and 4.2 μm. We quantify the design space available to these structures in terms of the ability to engineer and optimise the optoelectronic properties, and quantify the potential of metamorphic $InN_y(As_{1-x}Sb_x)_{1-y}$ structures for the development of mid-infrared light emitters, providing guidelines for the design of optimised light-emitting diodes.**

I. Introduction

Mid-infrared light-emitting diodes (LEDs) and lasers operating in the first atmospheric window, at wavelengths between 3 and 5 μm, are of importance for a range of practical applications including monitoring of trace gases and atmospheric pollutants, control of chemical processes, and free-space optical communications [1]. Generally, mid-infrared LEDs and lasers are based on GaSb or InAs substrates, which are both more expensive and less technologically mature compared to the GaAs- and InP-based platforms employed in near-infrared optical communications. LEDs and lasers operating between 3 and 5 μm are generally limited by optical and electrical losses, which are generally associated with the use of either (i) type-I quantum wells (QWs) having relatively low band offsets, so that thermal leakage of carriers significantly limits performance at and above room temperature, or (ii) type-II QWs, which have reduced optical efficiency. Recently, it has been demonstrated that utilising growth on $Al_zIn_{1-z}As$ metamorphic buffer layers (MBLs) provides a potential route to overcoming these limitations, since it allows for the growth of QWs having large type-I band offsets, thereby delivering high optical efficiency and suppressed thermal leakage at emission wavelengths between 3 and 4 μm [2].

We present a theoretical analysis and optimisation of the properties and performance of 3.3 and 4.2 μm LEDs based on metamorphic $InN_y(As_{1-x}Sb_x)_{1-y}/Al_zIn_{1-z}As$ QWs. We quantify the design space available to these structures, demonstrating that 3.3 μm emission can be readily achieved in N-free QWs having large type-I band offsets, whose properties can be engineered to enhance the spontaneous emission (SE) rate at fixed wavelength. In particular, we identify that optimum performance can be achieved via the use of tensile strained $Al_zIn_{1-z}As$ barriers, which has the potential to mitigate growth-related issues pertaining to strain-thickness limitations, and enable growth of high quality strain-balanced multi-QW structures. While our calculations indicate that the wavelength range accessible using $InAs_{1-x}Sb_x/Al_zIn_{1-z}As$ QWs is constrained to $\lesssim 4$ μm by strain-thickness limitations and carrier confinement [2], we predict that incorporation of dilute concentrations of nitrogen (N) is sufficient to push the emission wavelength beyond 4 μm in strain-balanced dilute nitride $InN_y(As_{1-x}Sb_x)_{1-y}/Al_zIn_{1-z}As$ structures.

II. Theoretical model

Our theoretical model of the optoelectronic properties of $InN_y(As_{1-x}Sb_x)_{1-y}/Al_zIn_{1-z}As$ metamorphic heterostructures is based on a 10-band **k·p** Hamiltonian for the $InN_y(As_{1-x}Sb_x)_{1-y}$ band structure. This model employs a conventional 8-band basis set of zone-centre conduction and valence band (CB and VB) edge Bloch states – including the spin-degenerate lowest energy CB, as well as the light-hole (LH), heavy-hole (HH) and spin-split-off (SO) VBs – which is augmented by the inclusion of a spin-degenerate N-related localised state [3]. The N-related states are resonant with and couple to the CB states of the $InAs_{1-x}Sb_x$ host matrix semiconductor: their impact on the band structure is taken into account in the 10-band model via a band-anticrossing interaction [4]. The parameters of the $InN_y(As_{1-x}Sb_x)_{1-y}$ **k·p** Hamiltonian have been determined via atomistic alloy supercell electronic structure calculations, and describe quantitatively the evolution of the main features of the band structure determined from experimental measurements [4].

The QW electronic properties are computed in the envelope function approximation: the numerical calculation of the QW eigenstates proceeds via a reciprocal space plane wave expansion method, which provides a robust and numerically efficient platform for the analysis of the electronic and optical properties [5]. The SE spectrum at fixed temperature ($T = 300$ K) and sheet carrier density ($n_{2D} = 10^{11}$ cm^{-2}) is calculated explicitly using the QW band structure, eigenstates and (quasi-equilibrium) carrier distribution functions, thereby accounting for the key effects of strain and N-induced hybridisation [2], [3]. We quantify the performance of candidate LED structures by computing the radiative current density, and identify optimised structures by maximising the radiative recombination coefficient B at the desired emission wavelength.

III. Results

Based on recently established epitaxial growth, we consider structures grown on $Al_{0.125}In_{0.875}As$ MBLs [2]. To target 3.3 μm emission we focus on N-free $InAs_{1-x}Sb_x/Al_zIn_{1-z}As$ QWs, where we constrain the Sb composition x in the compressively strained QW layers and Al composition z in

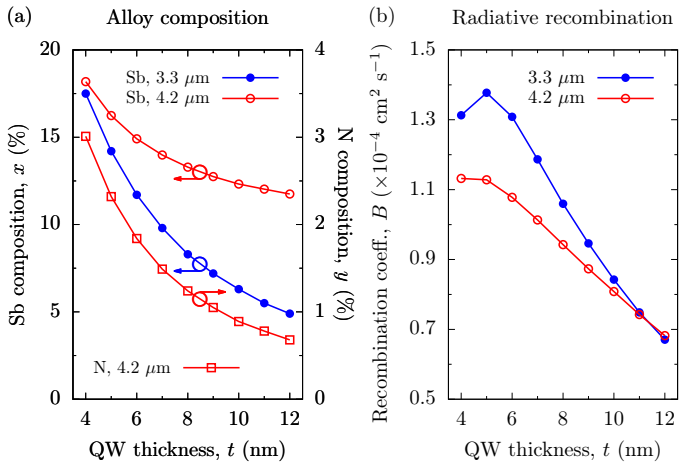

Fig. 1. (a) Variation with QW thickness t of the Sb and N compositions x (circles) and y (squares) required to achieve 3.3 μm (closed blue symbols) and 4.2 μm (open red symbols) emission at $T = 300$ K in strained-balanced $InN_y(As_{1-x}Sb_x)_{1-y}/Al_zIn_{1-z}As$ QWs grown on $Al_{0.125}In_{0.875}As$ MBLs. (b) Calculated variation of the radiative recombination coefficient B with QW thickness t in the N-free (3.3 μm; closed blue circles) and dilute nitride (4.2 μm; open red circles) QWs described by (a).

the tensile strained barrier layers to (i) obtain the peak of the SE spectrum at 3.3 μm, and (ii) produce overall strain-balancing by choosing x and z, as well as the corresponding QW and barrier thicknesses, to produce zero net in-plane stress in the structure [2]. Repeating this procedure as a function of the QW thickness t, we identify strain-balanced structures emitting at 3.3 μm. To achieve 4.2 μm emission we consider N-containing QWs, where dilute N compositions $y \lesssim 3\%$ are required to achieve emission wavelengths $\gtrsim 4$ μm. Our analysis centres on strain-balanced structures consisting of compressively strained $InN_y(As_{1-x}Sb_x)_{1-y}$ QWs, again having tensile strained $Al_zIn_{1-z}As$ barriers.

Figure 1(a) shows the Sb and N compositions x and y required to achieve room temperature emission at 3.3 and 4.2 μm, as a function of the QW thickness t. The range of Sb compositions required to achieve 3.3 μm emission ranges from 17.5% in a narrow QW having $t = 4$ nm, to 4.9% in a wide QW having $t = 12$ nm. The increase in x required to maintain fixed emission wavelength with decreasing t is associated with the larger confinement energy in a narrower QW. The corresponding QW compressive strains vary from 2.0% at $t = 4$ nm, to 1.2% at $t = 12$ nm. At 4.2 μm we consider QWs having a fixed compressive strain of 1.5%. We note that higher Sb compositions are required – in addition to N incorporation – in order to reduce the QW band gap sufficiently to produce emission at 4.2 μm. The Sb composition x required to maintain 4.2 μm emission reduces with increasing t (as in the 3.3 μm structures), as does the N composition y. The difficulty associated with N incorporation during epitaxial growth mandates minimising y, which our calculations indcate can be achieved via growth of thicker QWs.

Figure 1(b) summarises the calculated optical properties of these 3.3 and 4.2 μm strain-balanced structures. Here, the radiative recombination coefficient B has been computed by (i) integrating over the calculated SE spectrum to obtain the radiative current density $J_{\rm rad}$, and (ii) writing $J_{\rm rad} = eBn_{\rm 2D}^2$ in the Boltzmann approximation [2]. In order to remove any explicit dependence on t, we present B in two-dimensional units. At 3.3 μm we calculate a maximum value $B = 1.38 \times 10^{-4}$ cm^2 s^{-1} for a narrow QW having $t = 5$ nm, which decreases by a factor of approximately two as t is increased to 12 nm. At 4.2 μm we find that B is generally lower than in the N-free 3.3 μm structures, reflecting the reduction in the peak SE rate associated with the reduced band gap and optical transition matrix elements [3]. As at 3.3 μm, we again calculate that B tends to decrease with increasing t, suggesting that narrower QWs having $t \approx 5$ nm are favourable from the perspective of maximising the radiative efficiency.

Overall, our analysis quantifies the competing effects influencing the QW optical properties: narrower QWs are favoured to enhance the radiative efficiency, while wider QWs are favoured to reduce the Sb and N compositions required to reach a given emission wavelength.

IV. Conclusion

We have performed a theoretical analysis and optimisation of the properties and performance of $InN_y(As_{1-x}Sb_x)_{1-y}$ QWs grown on $Al_{0.125}In_{0.875}As$ MBLs, demonstrating the large scope offered by these structures for the development of mid-infrared LEDs operating at 3.3 and 4.2 μm. We have defined rigorous criteria for the design of strain-balanced structures incorpoating compressively strained QWs and tensile strained barriers, which is expected to allow for growth of high quality multi-QW structures. Via a systematic analysis of these structures we have identified key trends in their properties and performance as functions of the QW alloy composition, thickness and strain, thereby identifying optimised structures suitable for epitaxial growth and experimental investigation. Overall, our analysis confirms the promise of these novel metamorphic heterostructures for the development of high performance mid-infrared LEDs, and provides guidelines for the realisation of optimised devices.

Acknowledgement

This work was supported by the European Commission via the Marie Skłodowska-Curie Innovative Training Network PROMIS (project no. 641899), by Science Foundation Ireland (SFI; project no. 15/IA/3082), and by the National University of Ireland (NUI; via the Post-Doctoral Fellowship in the Sciences, held by C.A.B.).

References

[1] A. Krier, Ed., *Mid-Infrared Semiconductor Optoelectronics*. Springer, 2007.

[2] E. Repiso, C. A. Broderick, R. Arkani, E. P. O'Reilly, P. J. Carrington, and A. Krier, "Optical properties of metamorphic type-I $InAs_{1-x}Sb_x/Al_yIn_{1-y}As$ quantum wells grown on GaAs for the mid-infrared spectral range," *submitted*, 2018.

[3] S. Tomić, E. P. O'Reilly, R. Fehse, S. J. Sweeney, A. R. Adams, A. D. Andreev, S. A. Choulis, T. J. C. Hosea, and H. Riechert, "Theoretical and experimental analysis of 1.3-μm InGaAsN/GaAs lasers," *IEEE J. Sel. Topics Quantum Electron.*, vol. 9, p. 1228, 2003.

[4] E. P. O'Reilly, A. Lindsay, P. J. Klar, A. Polimeni, and M. Capizzi, "Trends in the electronic structure of dilute nitride alloys," *Semicond. Sci. Technol.*, vol. 24, p. 033001, 2009.

[5] M. Ehrhardt and T. Koprucki, Eds., *Multiband Effective Mass Approximations: Advanced Mathematical Models and Numerical Techniques*. Springer, 2014.